

http://pubs.acs.org/journal/acsodf

Substrate Activated Conformal Deposition Through Interfacial Control by a Soft Energy Intensification Process for Functional Integration in High Performance Artificial Intelligence Computing

Alain E. Kaloyeros* and Barry Arkles



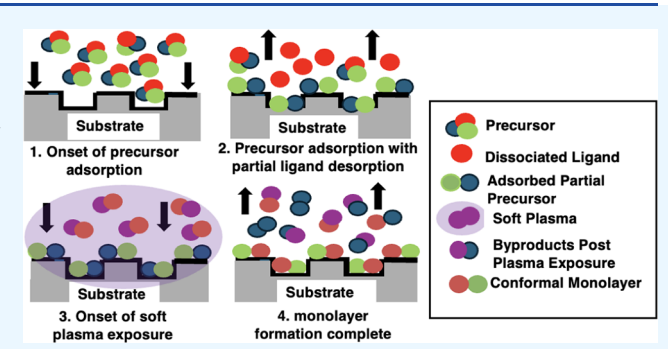
Cite This: ACS Omega 2025, 10, 23582-23590



ACCESS I

III Metrics & More

ABSTRACT: We demonstrate a soft energy vapor deposition process that enables atomic level control of the interface between the substrate surface and the growing multilayer film, while ensuring enhanced environmental sustainability and reduced energy consumption. The process combines the use of a low substrate temperature designed to induce selective ligand removal upon precursor interaction with the substrate surface, which we refer to as the "substrate surface activated" process, with the subsequent application of a soft plasma (ion energies below 5 eV and plasma power density below 0.05 W/cm²) that reacts with the adsorbed partially converted precursor species to complete the formation of a monolayer of the desired film. The soft plasma serves the additional



Article Recommendations

role of pretreating the substrate surface and the interface between the successive film monolayers to micromodulate the chemical reactivity and density of active surface atomic sites to maximize reaction efficiency, leading to elimination of any potential incubation period (nucleation delay). One advantage of this methodology is that the low temperature deposition enables the use of thermally or electrically fragile substrates. Other benefits include conformality in aggressive substrate surface topographies and significant decrease in energy consumption, leading to enhancement of growth rate per cycle. In this proof-of-concept study, cobalt tricarbonyl nitrosyl (Co(CO)₃NO) and 1,3,5-tri(isopropyl)cyclotrisilazane (TICZ, $C_0H_{27}N_3Si_3$) were employed as the source precursors for cobalt (Co) and silicon nitride (SiN), respectively. Cobalt was selected due to its current role as a conductor, liner, and cap layer in integrated circuitry (IC) metallization applications, while SiN was chosen given its multiple usages in IC technologies. Si_3N_4 and Co thin films were grown from the reaction of $Co(CO)_3NO$ with an argon (Ar) + 5 atom % hydrogen (H_2) plasma. In situ ellipsometry analyses demonstrated the effectiveness of the interfacial treatment in ensuring immediate film nucleation and elucidated the mechanisms of precursor-substrate surface interactions, leading to functional control of precursor decomposition pathways at low processing temperatures. X-ray photoelectron spectroscopy (XPS) investigations yielded stoichiometric Si₃N₄ and contaminant-free Co, while atomic force microscopy (AFM) shed light on the effects of post-deposition annealing on film microstructure and surface morphology.

1. INTRODUCTION AND BACKGROUND

Integrated circuitry (IC) technology roadmaps universally call for the heterogeneous integration in emerging system in package (SiP) architectures for high-performance artificial intelligence computing (HPC) of atomic elements and compounds that have not been previously employed in semiconductor systems. 1-3 They also stipulate the need for customized chemical process intensification techniques such as atomic layer chemical vapor deposition (ALCVD), atomic layer deposition (ALD), and molecular layer deposition (MLD) to grow these materials reliably and reproducibly, particularly at near-zero thicknesses.

As device design rules approach atomic scale and interelemental bonding dimensions, precise control of the thickness and composition of the materials that serve as IC building blocks becomes extremely critical. As a hypothetical illustration, for the 2 nm node, a 1 nm thick conducting film (such as copper or cobalt) would consist of no more than 15 to 20 atoms per layer, severely limiting any tolerances or variabilities in uniformity and conformality. In this respect, a cross-sectional variance of only a few atoms would likely cause the performance to move outside design specifications. As such, the concept of conformality is quickly moving from ±

Received: March 16, 2025 Revised: May 15, 2025 Accepted: May 19, 2025 Published: May 30, 2025





percentages to \pm atoms per layer. As a result, focus is shifting from traditional physical vapor deposition (PVD) and chemical vapor deposition (CVD) to chemical process intensification techniques. These chemically based molecular and atomic deposition processes actively interrogate the substrate surface to controllably modulate reactant adsorption and reaction mechanisms, thus providing excellent management of film composition, structure, and conformality.

The most common chemical process intensification techniques are ALD and ALCVD. Both methodologies are based on the concepts of 7-10 (i) sequential (nonconcurrent) delivery of precursor and coreactant pulses to the deposition chamber with intervening purge steps to ensure that reactions are limited to the substrate surface and are excluded from the gas phase and (ii) self-limiting precursor adsorption on the substrate surface in the form of an individual monolayer in every single pulse. In this manner, a near-zero-thickness film can be formed one monolayer at a time with precise thickness and exact uniformity. These atomically controlled techniques therefore ensure tight management of film thickness down to a few atoms along with enhanced conformality in subnanometer topographies and device features. 11,12 The fundamental distinction between ALD and ALCVD is the mechanism by which the precursor interacts with the substrate. In ALD, a chemical displacement reaction with specific functionality of the substrate takes place, while in ALCVD, the precursor undergoes a nonspecific chemical reaction, resulting in partial decomposition upon interaction with the substrate surface, which under ideal circumstances leads to lower deposition temperature and reduced cycle time. 13,14

Current ALD and ALCVD techniques suffer from inherent challenges that continue to limit their incorporation into IC manufacturing protocols. For one, typical growth rates are restricted to a few angstroms per cycle, which, compounded with the number of steps per cycle, severely hinders throughput and negatively impacts operational efficiency. The extended process time associated with the low growth rate per cycle is further exacerbated by a lag in the onset of actual film formation, commonly referred to as an "incubation period" or "nucleation delay". 15-17 Additionally, ALCVD methods are known to cause film contamination due to the occurrence of excessive precursor fragmentation in the vapor phase and the inability to limit the reaction solely to the substrate. Similarly, the deposition by thermal ALD and ALCVD of several elements and compounds of interest has been prohibited due to the need for markedly high temperatures to ensure efficient precursor conversion, well beyond what is acceptable in IC manufacturing. 18 Attempts to reduce processing temperatures through the application of a direct or remote plasma have been only partially successful due to the high plasma power densities applied, causing formation of porous low-density films, increased surface roughness, and the inclusion of contaminants by reaction or adsorption upon exposure to air. 19

We demonstrate in this report an operationally efficient process for conformal thin films that imposes a minimal energetic burden on the fabrication of nanoscale features consistent with the fragile structural elements of next-generation semiconductors. More specifically, we address the issues outlined above by developing a soft energy atomic vapor deposition intensification technique that enables atomic level control of the interface between the substrate surface and the growing multilayer film, while ensuring enhanced environ-

mental sustainability, reduced energy consumption, and successful integration into IC manufacturing flows. An important element of our process is the selection of a low substrate temperature that is adjusted to the activation energy required to affect the first step of a stepwise conversion of a precursor rather than causing complete precursor decomposition. This eliminates the "all-at-once" or immediate decomposition of a precursor, resulting in multiple decomposition products, creating pathways for film contamination.

In the process presented herein, as shown schematically in Figure 1, the substrate temperature is inherently low, given that

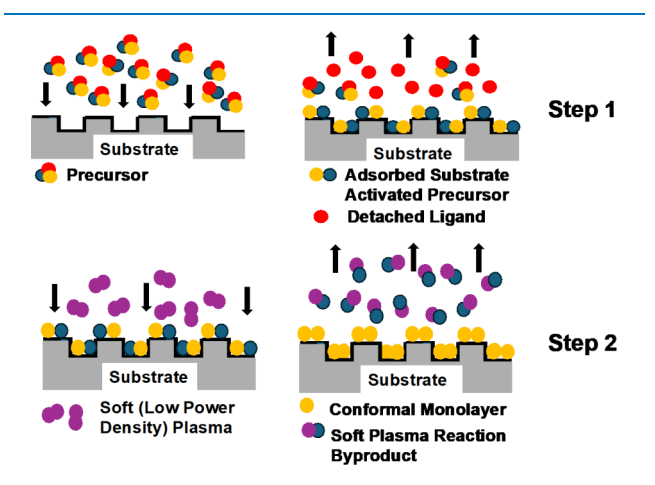


Figure 1. In step 1, the substrate temperature is adjusted to an activation energy required to induce selective ligand removal upon interaction of the precursor with the substrate surface without causing complete precursor decomposition. This substrate temperature is inherently low, given that it is intended to cause limited precursor fracture instead of decomposing the entire precursor, which we refer to as a "substrate activated" precursor. The resulting partially converted precursor forms a self-limiting conformal layer on the substrate. In step 2, the coreactant pulse (such as hydrogen or ammonia) consists of a soft (very low power density) direct or remote plasma. The soft remote or direct coreactant pulse (such as hydrogen or ammonia) consists of a soft (very low power density) direct or remote plasma. The soft remote or direct coreactant plasma reacts with the conformally adsorbed partial precursor species to form a monolayer of the desired film. Only a soft plasma (very low power density) is needed since the adsorbed precursor has already partially decomposed.

it is intended to cause only limited removal of substituents on the precursor upon interaction of the precursor with the substrate surface instead of decomposing the entire precursor. We refer to the substrate surface—precursor interaction as a "substrate activated" process. Concurrently, the low thermal budget ensures that the physisorbed or chemisorbed partial precursor species does not decompose uncontrollably, leading to a mixed composition and/or contaminated monolayer.

A second innovative aspect is that the precursor adsorption step is activated by the thermal energy and chemical structure of the substrate surface and not by a plasma. This enables the partial precursor species, after elimination of one or more ligands or attached radicals upon engagement with the substrate, to adsorb physically or chemically in a conformal fashion to various substrate surface topographies, including high-aspect ratio via trench structures. As a result, the subsequent application of a remote or direct coreactant plasma leads to the formation of the desired film that is conformal with

a uniform aspect ratio across the entire substrate surface, including highly aggressive device geometries.

Only a soft plasma (ion energies below 5 eV and plasma power density below 0.05 W/cm²) is needed since the adsorbed precursor has already been partially converted. The soft plasma serves the additional role of pretreating the substrate surface and the interface between the successive film monolayers to micromodulate the chemical reactivity and density of surface atomic sites to maximize reaction efficiency, leading to elimination of the incubation period (nucleation delay). We suggest that the plasma treatment and partial precursor decomposition maximize the concentration of active substrate surface sites and significantly decrease reaction activation energy, leading to elimination of nucleation delay and enhancement of growth rate per cycle. As such, the process is plasma-enabled, not plasma-enhanced or plasma-assisted. In the plasma-enabled process, the precursor pulse step is carried out thermally without the involvement of a plasma, while the coreactant pulse (for example, hydrogen or ammonia) is introduced in a soft direct or remote plasma. The soft remote or direct coreactant plasma then reacts with the adsorbed, partially converted precursor species to complete the conversion, forming a conformal monolayer of the desired film across the entire substrate surface, including in highly aggressive device geometries. The steps are then repeated multiple times until the desired thickness is achieved.

This report demonstrates the feasibility of the soft energy atomic vapor deposition process. Two of the most common conductor and dielectric building blocks of emerging IC architectures were selected, namely, cobalt (Co) and silicon nitride (SiN), as discussed in the subsequent sections. Co also serves as a liner and cap layer for copper (Cu)-based metallization schemes. The selection of both a single element and a binary compound is also aimed at emphasizing the diversity of the soft energy atomic vapor deposition process.

2. EXPERIMENTAL CONDITIONS

The precursors used in the soft energy atomic vapor deposition process are cobalt tricarbonyl nitrosyl ($Co(CO)_3NO$) and 1,3,5-tri(isopropyl)cyclotrisilazane (TICZ, $C_9H_{27}N_3Si_3$) for cobalt (Co) and silicon nitride (SiN), respectively. Relevant properties are listed in Table 1.

The precursor synthesis procedures have been previously reported. A 200 mm wafer PicoSun R200 research and development (R&D) deposition system was employed for all film processing experiments. The system consisted of two chambers: the first is a processing chamber with heated walls to a temperature well below the precursor thermal decomposition threshold to prevent undesirable reactant condensation, leading to film contamination, and the second is a load lock chamber with its outlet connected through a valving manifold to the deposition chamber. The two units are hermetically sealed with independently controlled environments using turbomolecular pump setups to ensure a continuously clean deposition environment that is tightly isolated from atmospheric contaminants. The system is equipped with a remote inductively coupled plasma (ICP) capability for plasma cleaning and plasma-enabled deposition. The substrates used consisted of 1000 nm-thick thermally grown silicon oxide on n-doped silicon wafers.

For SiN, the substrate was set at 200 °C, a temperature determined empirically and formulated to provide the thermal energy necessary for partial removal of alkyl groups (each with

Table 1. Chemical Structure and Pertinent Properties of Precursors Used

D	Duna a satu	Value
Precursor	Property	value
1,3,5-tri(isopropyl)cyclotrisilazane (TICZ, C ₈ H ₂₇ N ₃ Si ₃)	Chemical Structure	H ₂ Si Si N SiH ₂
	CAS Number	2013542-91-9
	Molar Mass	174.408 g/mol
	Appearance	Clear liquid
	Boiling Point	220-224 °C @ 1.8 torr
	Density	0.919 g/cm³ @ 20°C
	Melting Point	-69° to -71 °C
	Vapor Pressure	~1 torr @ 70°C
Cobalt tricarbonyl nitrosyl (Co(CO) ₃ NO)	Chemical Structure	0
	CAS Number	14096-82-3
	Molar Mass	172.969 g/mol
	Boiling Point	50 °C
	Appearance	Red oily liquid
	Density	1.47 g/cm ³ @20°C
	Melting Point	1.1 °C
	Vapor Pressure	~ 26 torr @ 0°C

a C–N bond energy of ~305 kJ) upon precursor monolayer adsorption to the substrate surface during the precursor pulse. This approach avoids breaking the Si–N ring and thus eliminates excessive precursor breakage, leading to ultimate film contamination. For the remote ammonia plasma pulse, the plasma power density was designed to reach ~0.05 W/cm² at the substrate surface, which provides the minimum activation energy necessary to complete breakage of the Si–N ring to form an uncontaminated SiN monolayer. The SiN deposition parameters are listed in Table 2. An extremely thin ZnO

Table 2. Deposition Parameters of the SiN Soft Energy Intensification Process Using TICZ as a Source Precursor

Parameter	Value
TICZ bubbler temperature	50 °C
Carrier gas	N ₂ @100 sccm
Substrate surface plasma pretreatment	NH_3
Incubation period (nucleation delay)	0.0 s (no delay)
Substrate temperature	200 °C
TICZ pulse duration	0.4 s
TICZ purge pulse	2.0 s
Purge gas	N_2
NH ₃ plasma pulse	10.0 s
NH ₃ flow rate	40 sccm
NH ₃ plasma power	2000 W
NH ₃ plasma power density	0.05 W/cm^2
NH ₃ purge pulse	3.0 s
Cycles	825
SiN film thickness	~44 nm
Capping layer	Extremely thin ZnO

capping layer was in situ deposited on top of SiN to act as a protective coating to prevent undesirable contamination upon exposure to air. The resulting SiN samples were split into two batches. One batch was analyzed as is, while the other batch was annealed in nitrogen at 400 °C for an hour prior to analysis. No structural, morphological, or compositional

differences were noted between the two batches. Accordingly, results are presented for the as-deposited samples.

For Co, the substrate was set at 200 °C, a temperature determined empirically and designed to provide the thermal energy necessary for partial removal of the carbonyl groups upon precursor monolayer adsorption to the substrate surface during the precursor pulse. This approach avoids breaking the Co–NO bond and thus eliminates excessive precursor breakage, leading to ultimate film contamination. For the remote H_2 plasma pulse, plasma power density was designed to reach $\sim 0.05 \ \text{W/cm}^2$ at the substrate surface, which provides the minimum activation energy necessary to complete the breakage of the Co–NO bond to form a clean Co monolayer. The Co deposition parameters are listed in Table 3.

Table 3. Deposition Parameters of the Co Soft Energy Intensification Process Using Cobalt Tricarbonyl Nitrosyl as a Source Precursor^a

Parameter	Value
Co bubbler temperature	Room temperature
Carrier gas	Ar@100 sccm
Substrate surface plasma pretreatment	$Ar + 5\% H_2$
Incubation period (nucleation delay)	0.0 s (no delay)
Substrate temperature	200 °C
Co pulse duration	0.1 s
Co purge pulse	1.0 s
Purge gas	Ar
H ₂ plasma pulse	5.0 s
$Ar + H_2$ flow rate	100 sccm
H ₂ plasma power	2000 W
H ₂ plasma power density	0.05 W/cm^2
H ₂ purge pulse	21 s
Cycles	300
Co film thickness	~30 nm
Capping layer	No cap

"The resulting Co samples were split into four batches. One batch was analyzed as is, while the other three were subjected to a different annealing recipe each. The three annealing recipes consisted of 1 h in 1 atm of Ar + 5% $\rm H_2$ at ~200 °C (recipe I), 1 h at ~300 °C (recipe II), and 1 h at ~450 °C (recipe III), respectively.

3. ANALYTICAL TECHNIQUES

Nonintrusive, real-time monitoring of experimental conditions, including nucleation and deposition mechanisms, was

performed using angle-resolved ellipsometry on a Woollam iSE ellipsometer with wavelengths in the range from 400 to 1000 nm. Quartz glass windows on the PicoSun system were employed to direct the incident light beam onto the substrate at an angle of 60.8° and reflect it at an equal angle to be acquired by a detector. Ellipsometry data were collected and analyzed by the software package CompleteEASE software, with the substrate being simulated as an ~1000 nm-thick thermal SiO₂ layer on Si. The SiO₂ thickness was determined in situ prior to every deposition run to ensure accurate simulation. Films' chemical bonding characteristics and quantitative elemental compositions were determined by Xray photoelectron spectroscopy (XPS) on a PHI Quantum 2000 system using a 1486.6 eV monochromated Al K α X-ray source. X-rays impinged on the samples at a $\pm 23^{\circ}$ incident angle and 45° reflection angle. Compositional analysis as a function of film thickness was carried out with an Ar⁺ ion gun at 2 keV, a 4×2 mm raster, and a 3.8 nm/min sputter rate. The Zn, Si, N, C, and O binding energies were well separated from each other, thus requiring no data deconvolution. CasaXPS software (Casa Software Ltd.) and MultiPak software (Ulvac-PHI) were employed to perform data processing and generate individual plots, respectively. Pre- and postannealing film roughness was analyzed by atomic force microscopy (AFM) on a Bruker Dimension Icon system equipped with a Nanoscope 6 controller. The system is equipped with a sample holder that can accommodate sample sizes of ≤2100 nm in diameter and ≤15 mm in thickness and has X-Y and Z ranges of 900 \times 900 and 100 nm, respectively.

4. RESULTS AND DISCUSSION

4.1. Ellipsometry Analysis. In the case of SiN, Figure 2 displays real-time, nonintrusive, in situ ellipsometry measurements of film thickness as a function of processing time at different substrate temperatures ranging from 30 to 200 °C. Significantly, as observed in the figure, the onset of thickness increases at t=0 corresponding to the first precursor pulse; film nucleation and growth begin instantaneously without the occurrence of an incubation period (nucleation delay).

This behavior is attributed to the low-power density plasma substrate surface pretreatment that enhances the density of chemically active atomic surface sites, associated with the minimal thermal budget provided by the low substrate temperature, causing partial precursor conversion and resulting in the formation of subprecursor species that are more reactive than the parent molecule when adsorbed to the substrate

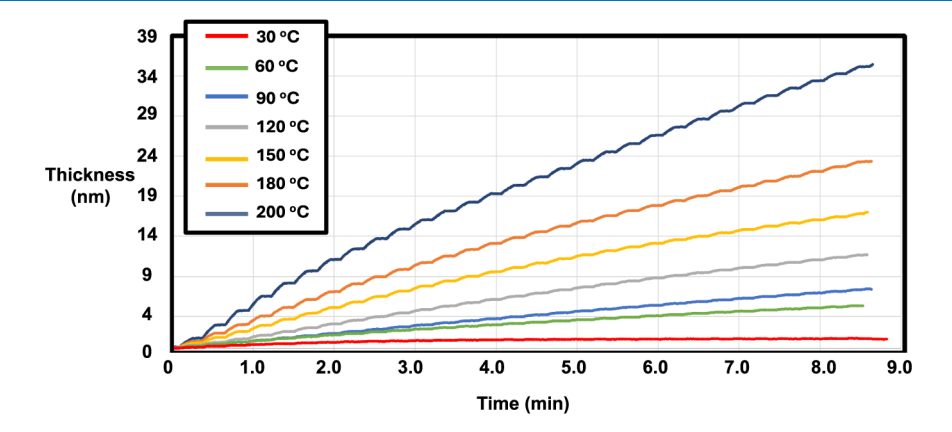


Figure 2. Real-time, in situ, nonintrusive ellipsometry profiles for SiN film thickness versus deposition time as a function of substrate temperature.

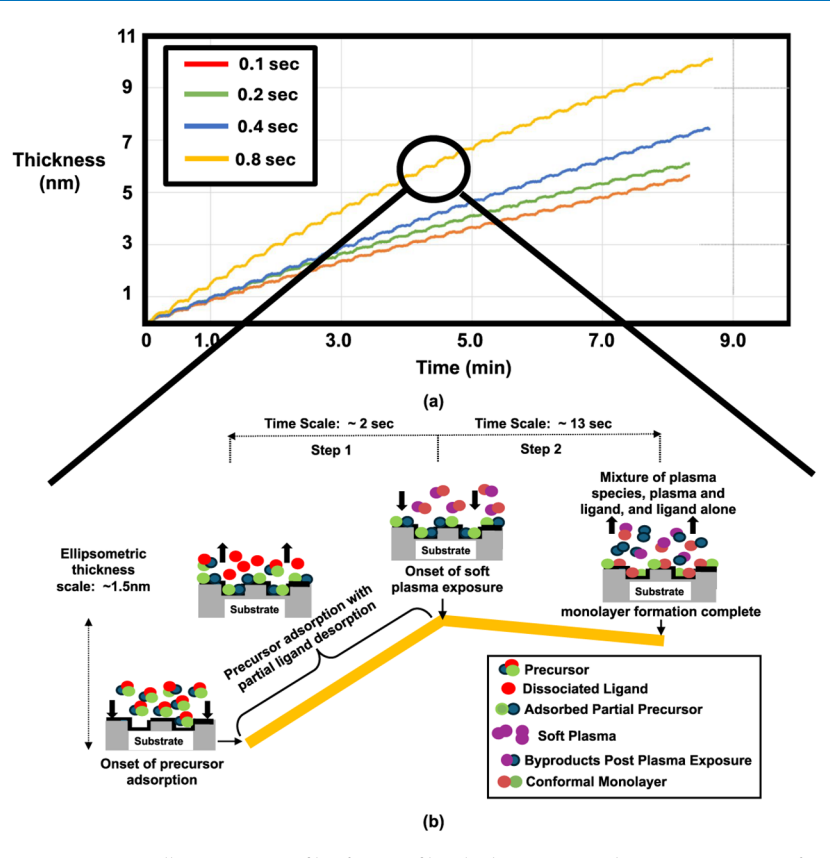


Figure 3. (a) Real-time, in situ, nonintrusive ellipsometry profiles for SiN film thickness versus deposition time as a function of precursor pulse time and (b) magnified schematic representation of an individual ripple or inflection cycle (represented by the solid orange lines) consisting of two reaction steps. Step 1 corresponds to the precursor adsorption and partial conversion upon interaction with the substrate surface, and step 2 relates to soft remote plasma reaction with the adsorbed "substrate activated" precursor to form a conformal SiN monolayer along with desorption of reaction byproducts.

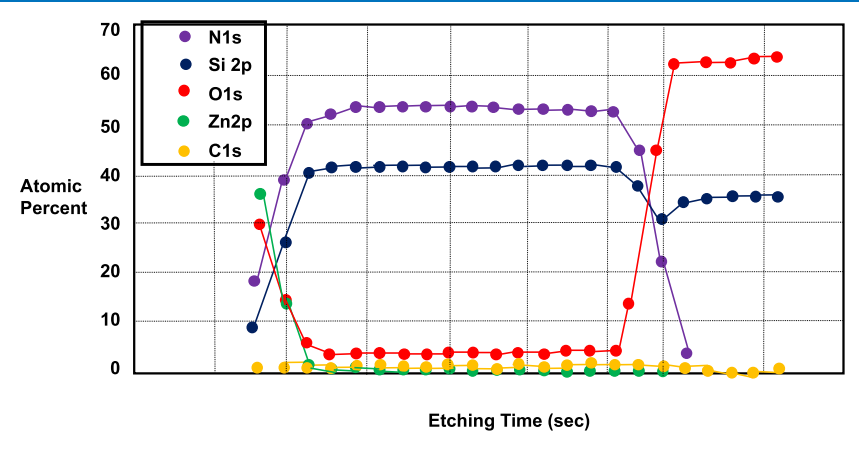


Figure 4. Typical XPS quantitative analysis of Zn, Si, N, C, and O elemental composition as a function of film thickness for SiN_x films grown at 200 °C substrate temperature.

surface. The combination of the two effects jointly causes a significant reduction in the reaction activation energy and results in the elimination of nucleation delay.

A second important conclusion can be derived from the SiN film deposition trend as a function of precursor pulse time, as shown in Figure 3. It is noted that the soft energy intensification process does not display a pure ALD mode since film thickness continues to increase with higher precursor pulse time and does not saturate, as would be anticipated in a pure ALD regime. This behavior is attributed to the first step in a stepwise decomposition of the precursor upon interaction

with the substrate surface. Similarly, the process does not exhibit a pure CVD process, given the monolayer-by-monolayer growth mode, as indicated by the rippled inflection-like profiles in Figures 2 and 3. Each ripple or pair of inflection points corresponds to a cycle consisting of one partially converted precursor adsorption step and a plasma reaction step, resulting in the formation of one SiN monolayer, as shown schematically in Figure 3. Instead, the soft energy intensification process is a hybrid ALD—CVD process without nucleation delay (lag in the onset of actual film formation and growth) and undesirable film contamination due to excessive

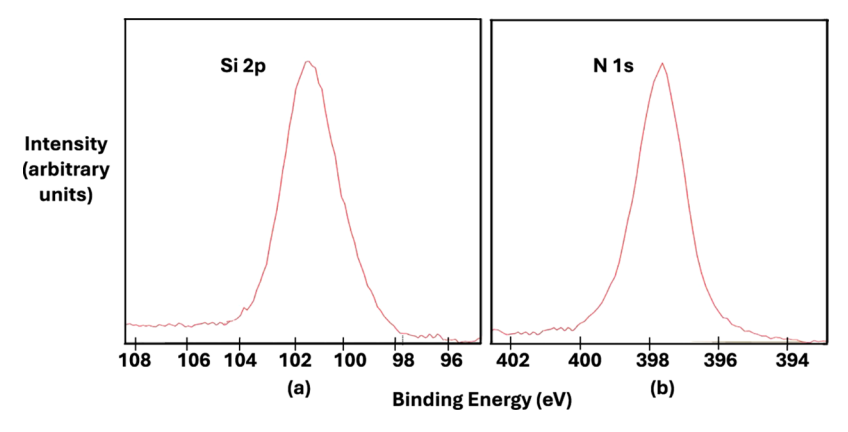


Figure 5. Typical SiN high-resolution XPS binding energy spectra for (a) Si 2p and (b) N 1s.

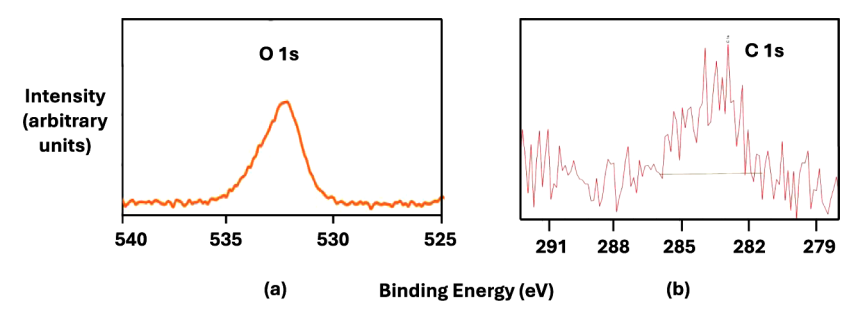


Figure 6. Typical SiN high-resolution XPS binding energy spectra for (a) O 1s and (b) C 1s.

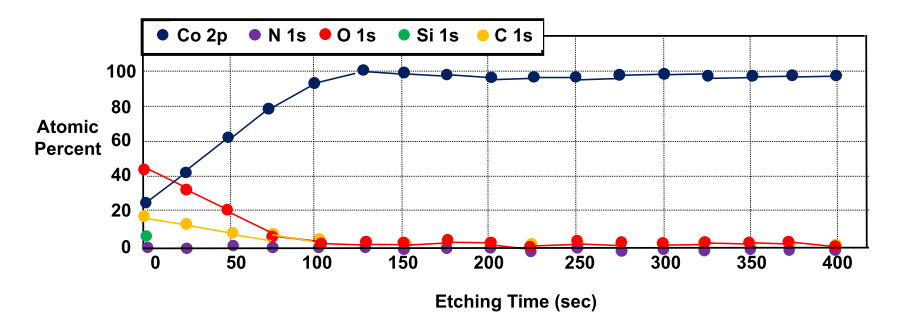


Figure 7. Typical XPS quantitative analysis of Co, Si, N, C, and O elemental composition as a function of film thickness for postannealed Co films grown as described in Table 3.

precursor fragmentation caused by uncontrollable reactions with the substrate. The same trends were observed in the soft energy process for the deposition of Co from cobalt tricarbonyl nitrosyl, supporting the occurrence of a hybrid low-temperature and low-plasma power density ALD—CVD process. The data are not shown due to their duplicative nature and for brevity.

4.2. XPS Analysis. Figure 4 presents the XPS quantitative analysis of Zn, Si, N, C, and O elemental composition as a function of film thickness for SiN_x films grown as described in Table 2 at a 200 °C substrate temperature. XPS yielded typical N and Si concentrations of ~54 and ~41.5 atom %, respectively, indicating a 4/3 N/Si compositional ratio and a stoichiometric Si_3N_4 phase. O and C concentrations were ~3.5 at % and below the detection limits of XPS, respectively. O inclusion was quite minimal and could be attributed to impurities in the carrier gas stream and/or plasma etching of the Al_2O_3 dielectric liners used to contain the plasma in the ICP plasma source. 25,26 Also, Figure 5a,b displays the high-resolution XPS spectra for Si 2p and N 1s binding energies in

SiN, respectively.²⁷ The Si 2p (\sim 101.8 eV) and N 1s peak (\sim 397.6 eV) locations and shape, including full-width-at-half-maximum (fwhm), are indicative of a stoichiometric Si₃N₄ phase, in support of the findings from XPS quantitative analysis.²

Also, Figure 6a,b displays the high-resolution XPS spectra for the O 1s and C 1s binding energies, respectively. The O 1s peak located at ~532.5 eV could be attributed to Si-O and/or N-O bonding arrangements. Alternatively, the C 1s peak is at the background noise level within the XPS detection limits, supporting the conclusion that C contaminants are absent in the SiN films.

Figure 7 presents the XPS quantitative analysis of Co, Si, N, C, and O elemental composition as a function of film thickness for postannealed Co films at 200 $^{\circ}$ C substrate temperature. XPS yielded a typical Co concentration of \sim 100 at %. O and C concentrations were below the detection limits of XPS.

Figure 8a,b displays the high-resolution XPS spectra for Co 2p binding energies in the Co films grown by the soft energy intensification process and the Co standard, respectively. Both

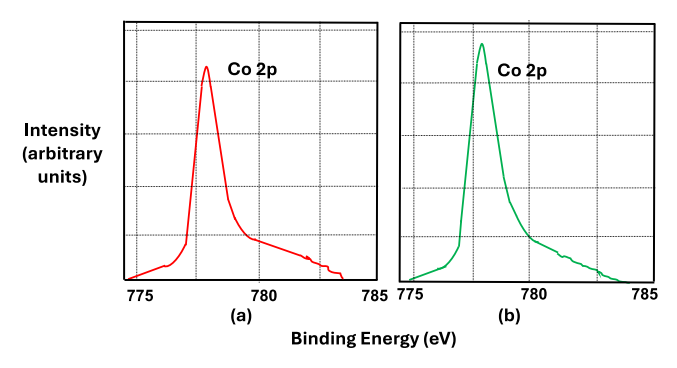


Figure 8. Typical high-resolution XPS binding energies spectra for (a) postannealed Co thin films deposited as described in Table 3I and (b) Co standard.

profiles exhibit the same characteristic shape of the Co 2p 3/2 photoelectron structure consisting of a main peak located at \sim 785 eV and a shoulder located at \sim 780.3 eV. This finding supports the result from XPS quantitative analysis, indicating high-purity cobalt.

4.3. AFM Analysis. The SiN samples' annealing experiments did not yield any structural or morphological differences from the as-deposited samples and will not be presented herein for the sake of brevity. The Co annealing experiments did not yield any structural or morphological differences from the asdeposited samples for annealing recipes I (200 °C) and II (300 °C), as shown in Figure 9a. However, samples annealed using recipe III (450 °C) exhibited marked changes in the form of significantly larger grain size, increased surface roughness, and a high void density, as shown in Figure 9b, where R_a is the root-mean-square surface roughness and the dimensions listed represent the XY coordinates' scan size. This behavior could be attributed to the availability of increased thermal energy at 450 °C, thus providing higher activation energy for Co grains to coalesce and grow into larger structures. This finding could have negative implications for the incorporation of Co into legacy (older generation) multilevel metallization schemes in

integrated circuitry (IC) process flows, given that the thermal budget for post-Co deposition manufacturing steps tends to exceed 450 °C and could therefore lead to poor grain morphology. For emerging IC architectures, however, the inclusion of thermally and electrically fragile materials, such as polymers, limits the thermal budget for post-Co deposition manufacturing steps to well below 450 °C, thus negating any concerns pertaining to Co film morphology.

5. CONCLUSIONS

This report describes the development of a soft energy atomic vapor deposition process that enables atomic level control of the interface between the substrate surface and the growing multilayer film, while ensuring enhanced environmental sustainability and reduced energy consumption. Adaptation of this technique is consistent with IC manufacturing flows for heterogeneous integration in emerging system in package (SiP) architectures for high-performance artificial intelligence computing. The process combines the use of a low substrate temperature designed to induce selective ligand removal upon precursor interaction with the substrate surface, which we refer to as the "substrate surface activated" process, with the subsequent application of a soft plasma (very low ion energies below 5 eV and plasma power density below 0.05 W/cm²) that reacts with the adsorbed partially converted precursor species to complete the formation of a monolayer of the desired film. The soft plasma serves the additional role of pretreating the substrate surface and the interface between the successive film monolayers to micromodulate the chemical reactivity and density of active surface atomic sites to maximize reaction efficiency, leading to elimination of the incubation period (nucleation delay) that has plagued atomic layer deposition. The process represents an extension and experimental validation of the important foundational theoretical work in the field.^{28–30} Carrying out the precursor pulse step under a thermally controlled environment ensures that the stepwise physisorbed or chemisorbed conversion of precursor species

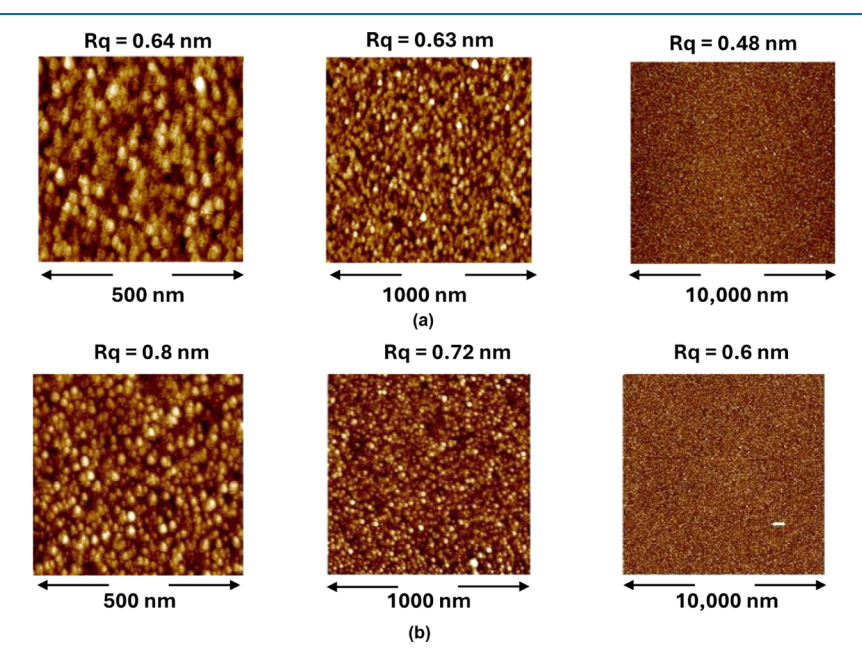


Figure 9. AFM scans of Co sample: (a) as deposited and (b) annealed at 450 °C indicate significantly larger grain size and increased surface roughness after the annealing step.

occurs conformally in various substrate surface topographies, including a high aspect ratio via trench structures, while the very low plasma power density avoids excessive precursor fragmentation, leading to a contaminated monolayer. It is also suggested that the plasma treatment and the formation of more reactive precursor subspecies due to selective precursor partial conversion maximize the concentration of active substrate surface sites and significantly decrease reaction activation energy, leading to elimination of any nucleation delay and enhancement of growth rate per cycle. A demonstration of feasibility of the soft energy atomic vapor deposition process was performed by selecting two of the most common conductors, liner, and cap layer (Co) and dielectric (SiN) building blocks of emerging IC architectures. The selection of a single element and a binary compound was also aimed at emphasizing the diversity and universality of the soft energy atomic vapor deposition process. For this work, the precursors used were cobalt tricarbonyl nitrosyl (Co(CO)₃NO) and 1,3,5-tri(isopropyl)cyclotrisilazane (TICZ) for cobalt (Co) and silicon nitride (SiN), respectively. The resulting research led to the identification of soft energy atomic vapor deposition processes for pure Si₃N₄ and Co thin films at 200 °C. Follow up investigations will focus on the demonstration of conformal near-zero thickness Si₃N₄ and Co layers in nanoscale topographies for heterogeneous integration in emerging system in package (SiP) architectures for high performance computing (HPC). The soft energy deposition process demonstrated here is anticipated to be broadly applicable, enabling previously unobtainable device structures of utility in IC fabrication. Additionally, with device design rules nearing atomic scale and layer thicknesses reaching 2 nm and below, atomic layer-based deposition methodologies such as the hybrid ALD-CVD process developed by the present investigators become increasingly competitive in terms of wafer throughput, production output, and operating expenses. However, scaling and eventual industrial adoption of such process intensification techniques face a few challenges that currently hinder the successful technology transfer from "lab to fab." One limiting factor is the disparity between research-scale process development in R&D tools and full-scale industrial manufacturing protocols in high volume fabrication (FAB) equipment. Another obstacle is the availability of relevant test structures with sub-4 nm high aspect ratios, which tend to be constrained to the top-tier IC manufacturers. The current investigators plan to collaborate with selected top-tier IC manufacturers to resolve these issues.

AUTHOR INFORMATION

Corresponding Author

Alain E. Kaloyeros — Kalark Nanostructure Sciences Inc., Doylestown, Pennsylvania 18902, United States; orcid.org/0000-0002-6872-1707; Email: Akaloyeros@kalarknano.com

Author

Barry Arkles – Kalark Nanostructure Sciences Inc., Doylestown, Pennsylvania 18902, United States; Chemistry Department, Temple University, Philadelphia, Pennsylvania 19122, United States

Complete contact information is available at: https://pubs.acs.org/10.1021/acsomega.5c02453

Funding

This work was funded by Kalark Nanostructure Sciences, Inc.

The authors declare no competing financial interest.

ACKNOWLEDGMENTS

The authors would like to thank Professor Spyros Gallis and Alexander E. Kaloyeros for their assistance with sample analysis. The authors would also like to recognize M. Patchés and B. Roo for their valuable input.

REFERENCES

- (1) Microelectronics and Advanced Packaging Technologies Roadmap. Semiconductor Research Corporation. 2023, https://srcmapt.org.
- (2) Manufacturing Roadmap for Heterogeneous Integration and Electronics Packaging 2023, UCLA Chips and SEMI USA. 2023. https://chips.ucla.edu/page/MRHIEP/MRHIEPFinalReport.
- (3) International Roadmap For Devices And Systems. IEEE. 2023, https://irds.ieee.org.
- (4) Oke, J.; Jen, T. C. Atomic layer deposition thin film techniques and its bibliometric perspective. *Int. J. Adv. Des. Manuf. Technol.* **2023**, 126, 4811–4825.
- (5) Park, J.; Kwak, S. J.; Kang, S.; Oh, S.; Shin, B.; Noh, G.; Kim, T. S.; Kim, C.; Park, H.; Oh, S. H.; et al. Area-selective atomic layer deposition on 2D monolayer lateral superlattices. *Nat. Commun.* **2024**, *15*, 2138–2148.
- (6) Vasilyev, V. Y. Atomic Layer Deposition of Silicon Dioxide Thin Films. ECS J. Solid State Sci. Technol. 2021, 10, 053004–053026.
- (7) Kaloyeros, A. E.; Goff, J.; Arkles, B. Emerging Molecular and Atomic Level Techniques for Nanoscale Applications. *Electrochem. Soc. Interface* **2018**, 27 (4), 59–65.
- (8) Zhang, L.; Liu, Z.; Ai, W.; Chen, J.; Lv, Z.; Wang, B.; Yang, M.; Luo, F.; Wu, J. Vertically grown metal nanosheets integrated with atomic-layer-deposited dielectrics for transistors with subnanometre capacitance-equivalent thicknesses. *Nat. Electron.* **2024**, *7*, 662–670.
- (9) Jain, A.; Pal, S.; Li, S.; Abbott, N. L.; Yang, R. Single-step synthesis of shaped polymeric particles using initiated chemical vapor deposition in liquid crystals. *Sci. Adv.* **2024**, *10* (45), 1–13.
- (10) Joo, S.; Seong, A.; Kwon, O.; Kim, K.; Lee, J. H.; Gorte, R. J.; Vohs, J. M.; Han, J. W.; Kim, G. Highly active dry methane reforming catalysts with boosted in situ grown Ni-Fe nanoparticles on perovskite via atomic layer deposition. *Sci. Adv.* **2020**, *6* (35), 1–8.
- (11) Xie, J.; Liao, L.; Gong, Y.; Li, Y.; Shi, F.; Pei, A.; Sun, J.; Zhang, R.; Kong, B.; Subbaraman, R.; et al. Stitching h-BN by atomic layer deposition of LiF as a stable interface for lithium metal anode. *Sci. Adv.* **2017**, 3 (11), No. eaao3170.
- (12) Si, M.; Lin, Z.; Chen, Z.; Sun, Y.; Wang, H.; Ye, P. D. Scaled indium oxide transistors fabricated using atomic layer deposition. *Nat. Electron.* **2022**, *5*, 164–170.
- (13) Wang, D.; Zhou, C.; Filatov, A. S.; Cho, W.; Lagunas, F.; Wang, M.; Vaikuntanathan, S.; Liu, C.; Klie, R. F.; Talapin, D. V. Direct synthesis and chemical vapor deposition of 2D carbide and nitride MXenes. *Science* **2023**, 379 (6638), 1242–1247.
- (14) Arkles, B.; Brick, C.; Goff, J.; Kaloyeros, A. E. A Simplified CVD Route to Near-Zero Thickness Silicon Nitride Films. *J. Vac. Sci. Technol. B* **2022**, *40*, 040601.
- (15) Yamaguchi, J.; Sato, N.; Tsukune, A.; Momose, T.; Shimogak, Y. Atomic Layer Deposition of Cobalt Film from Dicobalthexacarbonyl-tert-butylacetylene and Hydrogen. *ECS J. Solid State Sci. Technol.* **2023**, 12, 114003–114014.
- (16) Liu, J.; Lub, H.; Zhang, D. W.; Nolan, M. Self-limiting Nitrogen/Hydrogen Plasma Radical Chemistry in Plasma-Enhanced Atomic Layer Deposition of Cobalt. *Nanoscale* **2022**, *14*, 4712–4725. (17) Shima, K.; Otaka, Y.; Sato, N.; Funato, Y.; Fukushima, Y.; Momose, T.; Shimogaki, Y. Kinetic study on heterogeneous nucleation and incubation period during chemical vapor deposition. *J. Chem. Phys.* **2023**, *158*, 124704–124711.

- (18) Arkles, B.; Brick, C.; Goff, J.; Kaloyeros, A. E. A Simplified CVD Route to Near-Zero Thickness Silicon Nitride Films. *J. Vac. Sci. Techn. B* **2022**, *40*, 040601.
- (19) Boris, D. R.; Wheeler, V.; Nepal, N.; Qadri, S.; Walton, S. G.; Eddy, C. R. The role of plasma in plasma-enhanced atomic layer deposition of crystalline films. *J. Vac. Sci. Technol.* **2020**, A38, 040801–040841.
- (20) Arkles, B.; Brick, C.; Goff, J.; Kaloyeros, A. E. The low-temperature remote-plasma-activated pulsed chemical vapor deposition route to SiN_x from 1,3,5-tri(isopropyl)cyclotrisilazane. *Thin Solid Films* **2020**, 711, 138299.
- (21) Goff, B.; Brick, C. M.; Kaloyeros, A. E.; Arkles, B. Near-Room-Temperature Soft Plasma Pulsed Deposition of SiC_xN_y from 1,3,5-tri(isopropyl)cyclotrisilazane. *ECS Trans.* **2020**, 98, 121–135.
- (22) Diaz, C.; Pijper, E.; Olsen, R. A.; Busnengo, H. F.; Auerbach, D. J.; Kroes, G. J. Chemically Accurate Simulation of a Prototypical Surface Reaction: H₂ Dissociation on Cu(111). *Science* **2009**, 326, 832–834.
- (23) Eren, B.; Zherebetskyy, D.; Patera, L. L.; Wu, C. H.; Bluhm, H.; Africh, C.; Wang, L.-W.; Somorjai, A.; Salmero, M. Activation of Cu(111) surface by decomposition into nanoclusters driven by CO adsorption. *Science* **2016**, *351*, 475–478.
- (24) Opitz, J. "Electron impact ionization of cobalt-tricarbonyl-nitrosyl, cyclopentadienyl-cobalt-dicarbonyl and biscyclopentadienyl-cobalt: Appearance energies, bond energies and enthalpies of formation. *Int. J. Mass Spectrom.* **2003**, 225, 115–126.
- (25) Shih, H.-Y.; Lin, M.-C.; Chen, L. Y.; Chen, M.-J. Uniform GaN thin films grown on (100) silicon by remote plasma atomic layer deposition. *Nanotechnology* **2015**, *26*, 014002.
- (26) Motamedi, P.; Cadien, K. J. Structural and optical characterization of low-temperature ALD crystalline AlN. *Cryst. Growth* **2015**, 421, 45–52.
- (27) Moulder, J. F.; Stickle, W. F.; Sobol, P. E.; Bomben, K. D. Handbook of X-ray Photoelectron Spectroscopy. In *A Reference Book of Standard Spectra for Identification and Interpretation of XPS Data*; Chastain, J., Ed.; Perkin Elmer Corporation, Physical Electronics Division: Eden Prarie, MN, 1992.
- (28) Hou, H.; Gulding, S. J.; Rettner, C. T.; Wodtke, A. M.; Auerbach, D. J. The Stereodynamics of a Gas-Surface Reaction. *Science* **1997**, 277, 80–82.
- (29) Araujo, R. B.; Rodrigues, G. L. S.; dos Santos, E. C.; PetterssonL, L. G. M. Adsorption energies on transition metal surfaces: Towards an accurate and balanced description. *Nat. Commun* **2022**, *13*, 6853–6587.
- (30) Shirhatti, P. R.; Rahinov, I.; Golibrzuch, K.; Werdecker, J.; Geweke, J.; Altschäffel, J.; Kumar, S.; Auerbach, D. J.; Bartels, C.; Wodtke, A. M. Observation of the adsorption and desorption of vibrationally excited molecules on a metal surface. *Nat. Chem.* **2018**, 10, 592–598.